Research Article

Functional analysis of an upregulated calmodulin gene related to the acaricidal activity of curcumin against *Tetranychus cinnabarinus* (Boisduval)

Hong Zhou,[†] [ID] Fuyou Guo,[†] Jinxiang Luo, Yongqiang Zhang, Jinlin Liu, Yanchun Zhang, Xinyu Zheng, Fenglin Wan and Wei Ding[*]

Abstract

BACKGROUND: Curcumin is a promising botanical acaricidal compound with activity against *Tetranychus cinnabarinus*. Calmodulin (CaM) is a key calcium ion (Ca^{2+}) sensor that plays a vital role in calcium signaling. Overexpression of the *CaM* gene with inducible character occurs in curcumin-treated mites, but its functional role remains to be further analyzed by RNA interference (RNAi) and protein expression.

RESULTS: A CaM gene was cloned from *T. cinnabarinus* (designated *TcCaM*). *TcCaM* was upregulated and the protein was activated in mites by curcumin. The susceptibility of mites to curcumin was decreased after inhibiting *CaM* function with anti-CaM drug trifluoperazine (TFP) and silencing *CaM* transcription with RNAi, suggesting that the *CaM* gene is involved in the acaricidal activity of curcumin against mites. Moreover, the TFP pre-treated Sf9 cells were resistant to curcumin-mediated increase in $[Ca^{2+}]i$ levels, indicating that CaM-mediated Ca^{2+} homeostasis was disturbed by curcumin. *TcCaM* was then re-engineered for heterologous expression in *Escherichia coli*. Strikingly, our results showed that the recombinant CaM protein was directly activated by curcumin via inducing its conformational changes, its half-maximal effective concentration (EC_{50}) value is 0.3 μmol L^{-1} *in vitro*, which is similar to curcumin against CaM-expressing Sf9 cells (0.76 μmol L^{-1}) *in vivo*.

CONCLUSION: These results confirm that the overexpressed *CaM* gene is involved in the acaricidal activity of curcumin, and the mode of action of curcumin may be via activating CaM function, and thereby disrupting Ca^{2+} homeostasis in *T. cinnabarinus*. This study highlights the novel target mechanism of new acaricides, promoting our understanding of the molecular mechanism of CaM-mediated acaricide targets in mites.
© 2020 Society of Chemical Industry

Supporting information may be found in the online version of this article.

Keywords: *Tetranychus cinnabarinus*; curcumin; calmodulin; RNAi; heterologous expression

1 INTRODUCTION

The carmine spider mite, *Tetranychus cinnabarinus*, is one of the principal global agricultural mite pests of arthropods, feedings on over 100 types of plants, such as cotton, beans, corn, wheat, sesame, sunflower, and tomato.[1–3] These mites are extremely difficult to prevent and control because of their high fertility and inbreeding rate, small size, short developmental duration, and strong pesticide resistance.[4] Thus far, control of *T. cinnabarinus* mainly relies on chemical acaricides or insecticides, including pyridaben, spiromesifen, etoxazole and avermectin. However, there are many issues associated with acaricides, including the development of resistance, threats to non-target organisms, and environmental contamination. Consequently, an environmentally friendly acaricidal compound with a novel target should be identified and advanced to address these issues.

Curcumin is extracted from the rootstock of the plant *Curcuma longa* and extensively used as a food preservative, colorant, spice, and additive in cosmetics and pharmaceutical preparations.[5, 6] In addition, studies have confirmed that curcumin has broad-spectrum pharmacological activities, such as acaricidal,[7] insecticidal,[8] antifungal,[9] anti-inflammatory,[10] antioxidant,[11] anti-Alzheimer's,[12] and anticarcinogenic[13] effects. In particular, our previous research discovered that curcumin has outstanding repellent, contact killing, and ovipositional inhibition effects against *T. cinnabarinus*.[7, 14] Moreover, several characteristic neurotoxicity symptoms, including excitement and spasm, were observed in mites exposed to curcumin, suggesting that

* Correspondence to: W Ding, College of Plant Protection, Southwest University, Chongqing 400715, P. R. China. E-mail: dwing818@163.com

† These authors contributed equally.

Institute of Pesticide Science, College of Plant Protection, Southwest University, Chongqing, P. R. China

curcumin is a neurotoxin for which internal cellular calcium ion (Ca^{2+}) acts a vital role as a second messenger.[15] We also investigated the transcriptome of *T. cinnabarinus* after exposure to curcumin. Interestingly, a gene expressing calmodulin (CaM), which may participate in the action model of curcumin, was significantly upregulated in *T. cinnabarinus*.[16] However, the functional roles of CaM in the acaricidal mechanism of curcumin remain unclear in *T. cinnabarinus*.

Calcium ions are central signaling molecules in neurons that regulate various biological functions, including neurotransmitter release, gene expression, and muscle contraction.[17] Many cytoplasmic Ca^{2+}-binding proteins mediate the intracellular actions of Ca^{2+}.[18] Among these Ca^{2+}-binding proteins, CaM is the most important; CaM is principally expressed in the brain and acts a vital role in various physiological functions such as gene transcription, muscle contraction and relaxation, and signal transduction.[19] Although CaM itself does not display any catalytic activity, it regulates the activity of numerous CaM-dependent enzymes, including phosphodiesterases (PDE), Ca^{2+}-Mg^{2+}-ATPase, protein kinases, phosphatases, and nitric oxide synthases (NOSs).[20] CaM consists of approximately symmetrical N- and C-terminal lobes (hereafter referred to as the N- and C-lobes) linked by a flexible helix.[21, 22] Each lobe can jointly bind two Ca^{2+} in the micromolar range via two EF-hand motifs.[23] Upon Ca^{2+} binding to either lobe, several hydrophobic residues exposed promote the interaction of CaM with a target sequence of a regulated enzyme.[23] Notably, evidence has shown that CaM can be considered a potential target for pest management; e.g. the insecticidal mechanism of tomatine against *Helicoverpa armigera* is mediated by CaM,[24] and specific antagonists of CaM mediated by trifluoperazine (TFP, a specific inhibitor of CaM) inhibit the production of sex pheromones in *Bombyx mori*.[25]

Better characterization of the molecular targets of curcumin in mites may help in gaining insight about the mode of action of curcumin and aid in the discovery and development of new acaricides with novel targets, such as CaM in mites, for pest management. Here, the identification and verification of CaM acting as a molecular target of curcumin in mites are described. We first sequenced and then phylogenetically analyzed and characterized the expression pattern of a gene expressing CaM; the interaction between curcumin and CaM was subsequently investigated. A reverse genetic study using leaf-mediated double-stranded RNA (dsRNA) feeding was then employed to examine the link between the *CaM* gene and the acaricidal mechanism of curcumin against *T. cinnabarinus*; a functional cytotoxicity assay using Sf9 cells overexpressing CaM was also performed. The current research first shows that curcumin is a novel agonist of CaM function and offers pivotal clues for elucidating the molecular mechanisms underlying the activity of curcumin against *T. cinnabarinus*.

2 MATERIALS AND METHODS

2.1 Mites
Tetranychus cinnabarinus was gained from cowpea (*Vigna unguiculata*) seedlings in Beibei, Chongqing, China.[16] Additionally, the mites were reared for over 17 years without any pesticides at 26 ± 1 °C, 70–75% relative humidity (RH), and a 14-h/10-h (light/dark) photoperiod. Collection of mites that are agricultural pests and widely distributed does not require a specific license.

2.2 [Ca^{2+}]i assay
Sf9 (*Spodoptera frugiperda*) cells were maintained at 27 ± 1 °C in Sf-900™ SFM culture medium (Gibco, California, USA). Because the cell lines of mites cannot be cultured *in vitro*, Sf9 cells were used for experiments and treated with curcumin (99%, Shanghai Yuanye Biotechnology, Shanghai, China) at concentrations of 0, 2.6, 8.2 and 53 $\mu mol\ L^{-1}$ (LC_{30}, LC_{50} and LC_{80}) for 48 h to detect the effect of curcumin on internal cellular [Ca^{2+}]i levels. Fluo-4/AM fluorescence staining (Beyotime Biotechnology, Shanghai, China) was used to measure [Ca^{2+}]i concentrations in the Sf9 cells, and the details of the [Ca^{2+}]i assay were described by Zhou *et al.*[26]

2.3 Bioassay
Curcumin toxicity against *T. cinnabarinus* was determined by the FAO-recommended slip-dip method.[27, 28] The sublethal concentrations of curcumin against mites were measured by log-probit analysis of bioassay data.[29] Each independent experiment consisted of three biological replicates. In the bioassay, the LC_{10}, LC_{30}, and LC_{50} values of curcumin were 0.21, 1.23, and 2.64 mg L^{-1}, respectively.

2.4 Total RNA extraction, cDNA synthesis, and *TcCaM* cloning
Female adult (3–5 days old) mites were used to extract total RNA with the RNeasy® plus Micro Kit (Tiangen, Beijing, China). The RNA quantity was determined at $OD_{260/280}$ using a Nanovue UV-visible spectrophotometer (GE Healthcare, Fairfield, CT, USA) and further validated by 1% agarose gel electrophoresis. Complementary DNA (cDNA) was synthesized using PrimeScript® 1st Strand cDNA Synthesis Kit (Takara, Dalian, China). The cDNA was stored at −20 °C.

Specific primers (Supporting Information Table S1) were designed and synthesized to obtain the DNA sequence of the CaM gene on the basis of the whole-genome sequence of the sister species *T. urticae*. Polymerase chain reactions (PCRs) were conducted with 10× PCR buffer (2.5 μL), $MgCl_2$ (2.5 μL), dNTPs (2.0 μL), cDNA template (1 μL), rTaq™ polymerase (0.2 μL), F/R primers (1 μL), and 14.8 μL doubled-distilled water (ddH_2O) to a final reaction volume of 25 μL. The PCR program consisted of 94 °C for 3 min, 35 cycles of 94 °C for 30 s, 55 °C for 30 s, and 72 °C for 50 s, and a final extension for 10 min at 72 °C. The PCR products were gel-purified using a Gel Extraction Mini Kit (Tiangen), ligated into the pMD™ 19-T vector (Takara), and transfected into *Escherichia coli* DH5α-competent cells (Tiangen) for sequencing at the Beijing Genomics Institute (Beijing, China).

2.5 Gene characteristic and phylogenetic analysis
The *CaM* gene sequence was edited with DNAMAN 5.2.2, and amino acid sequences were aligned via the ClustalW program.[30,31] The molecular weights and isoelectric points of the CaM protein were computed using ExPASy. A phylogenetic tree of *CaM* genes was built with MEGA 7.0 using the neighbor-joining (NJ) method via 1000 bootstrap replicates.[32]

2.6 RNAi
T7 promoter primers (Table S1) of the *CaM* gene were designed and synthesized to amplify target sequences. Green fluorescent protein (GFP) (ACY56286) was regarded as a negative control. The amplified products were gel-purified and dsRNA was synthesized using Transcript Aid T7 High Yield Transcription Kit (Thermo Scientific, Vilnius, Lithuania). The lengths of the dsRNA products were measured by agarose gel electrophoresis, and

concentrations were measured via spectrophotometry. The dsRNAs were stored at −70 °C. A leaf-disc dsRNA feeding method[28] was employed to silence *TcCaM* expression, and the details of the RNA interference (RNAi) assay were described in our previous study.[26]

2.7 Quantitative real-time PCR (qPCR)

Specific primers for quantitative real-time PCR (qPCR) were designed with Primer 5.0,[33] and *RPS18* was regarded as the reference gene,[34] as shown in Table S1. The qPCR was performed with the cDNA template (1 μL), iQ™ SYBR® Green Supermix (10 μL, BIO-RAD, Hercules, CA, USA), 0.2 mmol L^{-1} of each gene primer (1 μL), and ddH$_2$O (7 μL) to a final 20-μL reaction volume. The protocol of qPCR was 95 °C for 2 min, 40 cycles of 95 °C for 15 s, 60 °C for 30 s, and 72 °C for 30 s; melt curve analysis was performed (60 °C to 95 °C). Each independent experiment consisted of three technical and biological replicates. The $2^{-\Delta\Delta Ct}$ method was employed to quantify the expression levels of genes.[35]

2.8 Prokaryotic expression of the *CaM* gene

The procedure was essentially the same as that described by He *et al.*[36] Briefly, specific primers with restriction enzyme sites (BamHI and SmaI) were synthesized to amplify the coding region of *CaM* via PCR, as shown in Table S1. The PCR product was digested using the restriction enzymes BamHI and SmaI (Takara), gel purified, and ligated into the pGEX-6P-1 vector, which was further transfected into BL21 (DE3)-competent cells for CaM expression. After incubation for 12 h at 37 °C with shaking at 200 rpm, the cells were diluted at a ratio of 1:100 with Luria Bertani medium with 100 mg L^{-1} ampicillin and subsequently maintained at 37 °C to an OD$_{600}$ value of 0.6–0.8. The suspended cells were induced with 24 mg L^{-1} isopropyl *β*-D-1-thiogalactopyranoside and then cultured for 12 h under the earlier conditions. The fusion protein was purified using BeyoGold™ GST-tag Purification Resin (Beyotime Biotechnology, Beijing, China) and analyzed via sodium dodecyl sulfate-polyacrylamide gel electrophoresis (SDS-PAGE); the protein concentration was determined using the Bradford method.

2.9 CaM assay

Fluorescent labeling with dansyl chloride (Sigma, St Louis, MO, USA), PDE activity, Ca^{2+}-Mg^{2+}-ATPase activity were determined as a function of CaM concentration, respectively. Due to the weak endogenous fluorescence of CaM, dansyl chloride can be used as a fluorescent substance to label CaM (D-CaM).[37] When curcumin binds to D-CaM, the conformation of D-CaM changes, which increases the hydrophobicity and fluorescence of dansyl chloride. The interaction between curcumin and CaM was evaluated by studying the change in the fluorescence intensity at 340 nm of D-CaM caused by the addition of curcumin. PDE activity was assayed according to its ability to hydrolyze cAMP (Sigma) to 5′-AMP[38]; the 5′-nucleotidase (Sigma) degradation products adenosine and orthophosphate (Pi) were then measured by spectrophotometry at 660 nm.[39] Briefly, the assay was conducted using a BioTekmicroplate reader (BioTek, Winooski, VT, USA) at 37 °C in a reaction containing 50 μL phosphate-buffered saline (PBS, pH 7.4 and 0.04 mol L^{-1}), 25 μL CaCl$_2$ (4.5 mmol L^{-1}), 25 μL CaM protein, 100 μL cAMP (5 mmol L^{-1}), 20 μL PDE protein (5 μmol L^{-1}, Sigma), 20 μL 5′-nucleotidase (5 μmol L^{-1}), and 10 μL of a solution of a varying concentration of curcumin. The Ca^{2+}-Mg^{2+}-ATPase activity was determined by its ability to catalyze the hydrolysis of ATP to ADP and Pi.[40] The Ca^{2+}-Mg^{2+}-ATPase reaction was followed spectrophotometrically at 660 nm of a buffer containing 50 μL PBS (pH 7.4 and 0.04 mol L^{-1}), 25 μL MgCl$_2$ (4.5 mmol L^{-1}), 25 μL CaCl$_2$ (4.5 mmol L^{-1}), 25 μL CaM protein, 100 μL ATP (5 mmol L^{-1}), 25 μL Ca^{2+}-Mg^{2+}-ATPase (5 μmol L^{-1}, Sigma), and 10 μL of a solution of a varying concentration of curcumin. Each reaction had three replicates. The half-maximal effective concentration (EC$_{50}$) for the assay was calculated by SPSS (v.16.0, SPSS Inc., Chicago, IL, USA).

2.10 Functional expression and cytotoxicity assay

The Bac-to-Bac baculovirus system (Invitrogen, Carlsbad, CA, USA) was used to express CaM in Sf9 cells according to the manufacturer's protocol. Briefly, the coding region of CaM was ligated into the pFastBac HTA expression vector, which was further transfected into Sf9 cells. After culture for 72 h at 27 °C, the infected Sf9 cells were harvested and resuspended for evaluation of the activity of PDE activation by CaM.

MTT Cell Proliferation and Cytotoxicity Assay Kit (Solarbio, Shanghai, China) were used to measure the cytotoxicity of curcumin according to the manufacturer's protocol. Briefly, infected cells were pre-incubated for 24 h in a 24-well plate, and 10 μL of curcumin diluted in dimethyl sulfoxide (DMSO) at different concentrations (1.25, 2.5, 5, 10, 20 and 40 μmol L^{-1}) was added and incubated for 48 h. After the medium was removed, 200 μL fresh medium and 200 μL 3-(4,5-dimethyl-thiazol-2-yl)-2,5-diphenyltetrazolium bromide (MTT) solution were added to each well and incubated for 4 h. The solution was removed, 300 μL DMSO was added, and the mixture was mildly heated for 10 min. Absorbance was determined at 490 nm using BioTekmicroplate reader. As a control, the parental Sf9 cells were infected with a GFP-expressing baculovirus. Each treatment consisted of three technical and biological replicates. The half-maximal inhibitory concentration (IC$_{50}$) for the assay was calculated by SPSS (v.16.0, SPSS Inc.).

2.11 Molecular docking

Docking was evaluated using AutoDock 4.2. The three-dimensional (3D) model of *TcCaM* and its binding pocket were generated using the I-TASSER server (http://zhanglab.ccmb.med.umich.edu/I-TASSER/). The 3D model of the ligands was established, and their energy minimization was calculated by ChemOffice 2004.[41] The model results were analyzed by Discovery Studio Visualizer 4.5 (Accelrys Software Inc., San Diego, CA, USA).[42]

3 RESULTS

3.1 [Ca^{2+}]i assay

As a calcium indicator, the intracellular [Ca^{2+}]i concentrations were measured using Fluo-4/AM staining, as shown in Fig. 1. According to statistical analysis, after Sf9 cells incubated with curcumin at concentrations of LC$_{30}$ (2.6 μmol L^{-1}), LC$_{50}$ (8.2 μmol L^{-1}) with TFP-pre-treated (58 μmol L^{-1}, IC$_{50}$ dose of TFP), and LC$_{50}$ respectively for 48 h, the intracellular [Ca^{2+}]i levels were significantly higher (3.17-, 4.49-, and 8.05-fold, respectively) compared with the control, indicating the [Ca^{2+}]i levels in insect Sf9 cells were significantly increased by curcumin exposure in a concentration-dependent manner (Fig. 1). However, intracellular [Ca^{2+}]i levels were markedly attenuated in the TFP-pre-treated Sf9 cells.

3.2 cDNA cloning, characterization and phylogenetic analysis of *TcCaM*

The full-length cDNA sequences of *TcCaM* were obtained by PCR and submitted to GenBank (accession numbers: KY436226). *TcCaM* consists of an open reading frame (ORF) of 501 bp that
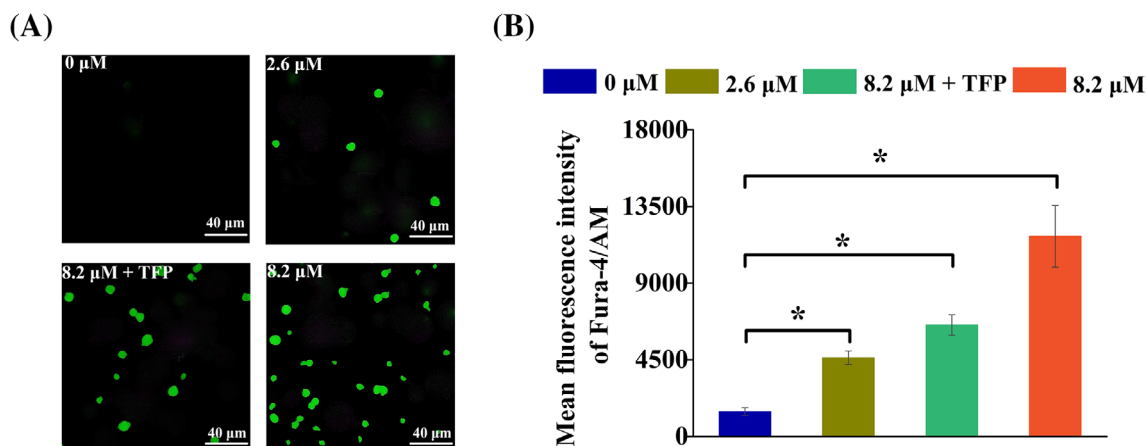
(A)   (B)

Figure 1. Effects of curcumin on intracellular free calcium [Ca²⁺]i levels in Sf9 cells. The 0, 2.6 and 8.2 µmol L⁻¹ indicate Sf9 cells incubated with curcumin at concentrations of 0, 2.6 and 8.2 µmol L⁻¹ (0, LC$_{30}$ and LC$_{50}$), respectively for 48 h; 8.2 µmol L⁻¹ + TFP indicates TFP-pre-treated (58 µmol L⁻¹, IC$_{50}$ dose of TFP) Sf9 cells incubated with curcumin at 8.2 µmol L⁻¹ (LC$_{50}$) for 48 h. (A) The [Ca²⁺]i level was detected by Fluo-4/AM fluorescence staining. Positively stained calcium is shown as green zones in the captured images under a microscope. (B) The bar chart indicates the mean fluorescence intensity of Fluo-4/AM in Sf9 cells. Error bars represent the standard error of the calculated mean based on three biological replicates. An asterisk (*) on the error bar indicates a significant difference between the treatment and group CK according to *t*-tests, *$P < 0.05$.

encodes a protein of 167 amino acids. The predicted isoelectric point of the *TcCaM* protein is 4.32, and the calculated molecular mass is 19.03 kDa. *TcCaM* is predicted to possess four EF-hand domains, as shown in Fig. 2(A).

Phylogenetic analysis was conducted on the basis of the amino acid sequence of *TcCaM* as well as the sequences of other CaM proteins, including in arachnids, insects and mammals. All CaM sequences with a complete ORF were obtained from the *T. urticae* genome and National Center for Biotechnology Information (Bethesda, MD, USA) (http://www.ncbi.nlm.nih.gov/) (Table S2). The results showed that *TcCaM* groups with other sequences from Arachnida and shares the highest genetic relationship with the CaM of *T. urticae* (*TuCaM*) (100% similarity, Fig. 2(B)), indicating likely analogous physiological functions between *TcCaM* and *TuCaM*.

3.3 Expression patterns of *TcCaM* in different developmental stages and curcumin exposure groups

The transcript levels of the *TcCaM* gene during different developmental stages (egg, larva, nymph, and female adult mites) and in different curcumin treatment groups (at the LC$_{50}$, LC$_{30}$, and LC$_{10}$ doses of curcumin) were evaluated via reverse transcription PCR (RT-PCR) and qPCR, respectively. To detect *TcCaM* gene expression throughout the different life stages of mites, approximately 2000 eggs, 1500 larvae, 800 nymphs, and 200 adults were collected per sample in triplicate. Relative expression of *TcCaM* in larvae, nymph, and adult mites was increased by 2.48-, 2.90-, and 3.09-fold compared with that in eggs, respectively (Supporting Information Fig. S1). The results indicated no significant difference in the expression levels of *TcCaM* in different developmental stages, except for egg stages, which were much lower.

Relative expression of the *TcCaM* of *T. cinnabarinus* exposed to LC$_{10}$, LC$_{30}$ and LC$_{50}$ curcumin (0.21, 1.23, and 2.64 mg L⁻¹) in 0.1% (v/v) Tween-80 and 3% (v/v) acetone at the adult stage for 48 h using a slip-dip bioassay were analyzed using RT-PCR and qRT-PCR, respectively. The results of the curcumin exposure experiment demonstrated that the *CaM* gene was upregulated at 48 h by curcumin treatment compared with the control [water containing 0.1% (v/v) Tween-80 and 3% (v/v) acetone], as shown

in Fig. 3(A). According to statistical analysis, at the LC$_{50}$, LC$_{30}$, and LC$_{10}$ doses of curcumin, relative expression levels of *TcCaM* were significantly higher (7.30-, 5.47-, and 3.91-fold, respectively) at 48 h compared with the control.

3.4 PDE activation by CaM and toxicity after curcumin and TFP exposure

The PDE activation by CaM of *T. cinnabarinus* exposed to curcumin LC$_{10}$, LC$_{30}$ and LC$_{50}$ (0.21, 1.23, and 2.64 mg L⁻¹) in 0.1% (v/v) Tween-80 and 3% (v/v) acetone was determined. At the LC$_{50}$, LC$_{30}$, and LC$_{10}$ doses of curcumin, the PDE activation by crude CaM was significantly higher (2.26-, 1.82-, and 1.45-fold higher, respectively) at 48 h compared with the control [water containing 0.1% (v/v) Tween-80 and 3% (v/v) acetone, Fig. 3(B)].

The PDE activation by CaM of *T. cinnabarinus* exposed to 58 µmol L⁻¹ TFP (IC$_{50}$) in 0.1% (v/v) Tween-80 and 3% (v/v) acetone at the adult stage was determined. Compared with the control [water containing 0.1% (v/v) Tween-80 and 3% (v/v) acetone, 152.57 nmol mg⁻¹ min⁻¹], the PDE activation by crude CaM (81.41 nmol mg⁻¹ min⁻¹) was inhibited *in vivo* by TFP treatment (58 µmol L⁻¹, IC$_{50}$ dose of TFP), and 46.64% of its activity was inhibited in mites after exposure to TFP for 48 h (Fig. S2).

When endogenous CaM was inhibited in *T. cinnabarinus* pre-treated with TFP (58 µmol L⁻¹, IC$_{50}$ dose of TFP), the toxicity of curcumin against adult females of *T. cinnabarinus* after 48 h curcumin exposure was determined. As shown in Table 1, the toxicity assays indicated that the LC$_{50}$ of curcumin against *T. cinnabarinus* (9.61 mg L⁻¹) was increased 3.64-fold compared with the control (2.64 mg L⁻¹).

3.5 Functional analysis of CaM by RNAi

For investigating the transcript knockdown efficiency of the *TcCaM* expression, relative messenger RNA (mRNA) expression levels were measured via RT-PCR and qRT-PCR at 48 h post-dsRNA feeding. The results showed that the transcript levels of *TcCaM* were significantly decreased by 62% after feeding with *TcCaM* dsRNA compared with feeding of diethyl pyrocarbonate (DEPC)–water or dsRNA–GFP (Fig. S3). No significant difference was found between the DEPC–water and dsRNA–GFP controls (Fig. S3).

(A)

```
1    ATGTTAAACGACTCCATGCATCCTGATCCTTGTGATACCAATTTACAGGCTGAATATGGCCTGACCCAGGAACAGATAGCTGAATTTC
1     M  L  N  D  S  M  H  P  D  P  C  D  T  N  L  Q  A  E  Y  G  L  T  Q  E  Q  I  A  E  F
91   GAGGCCTTTAGACTGTTTGATAAAGATTGCGATGGACGAATCACTTCAACTGAATTGGGTATTGTTATGAGATCTTTGGGTCAACGAG
31    E  A  F  R  L  F  D  K  D  C  D  G  R  I  T  S  T  E  L  G  I  V  M  R  S  L  G  Q  R
181  ACAGAAACTGAGCTCAAAAATATGGTCACTCTTGTTGACCAAGATGGAAATGGAACTATTGAATTCAATGAATTTCTTCACATGATGT
61    T  E  T  E  L  K  N  M  V  T  L  V  D  Q  D  G  N  G  T  I  E  F  N  E  F  L  H  M  M
271  CGTAAAATGAAGGAAACAGATAAAGAAGAGGAACTTCGAGAAGCTTTTAGAGTATTTGACAGGAATGGTGATGGTTTTATCAACGCTG
91    R  K  M  K  E  T  D  K  E  E  E  L  R  E  A  F  R  V  F  D  R  N  G  D  G  F  I  N  A
361  GAGTTAAGGCACGTTATGACCAATTTAGGGGAAAAATTGACCGACGAAGAGGTTGAAGATATGATTAAAGAGGCTGATCTGGATGGCG
121   E  L  R  H  V  M  T  N  L  G  E  K  L  T  D  E  E  V  E  D  M  I  K  E  A  D  L  D  G
451  GGTTTGGTCAATTATGATGAGTTTGTTAATGTTTTGATGGCACCTAAATGA
151   G  L  V  N  Y  D  E  F  V  N  V  L  M  A  P  K  *
```
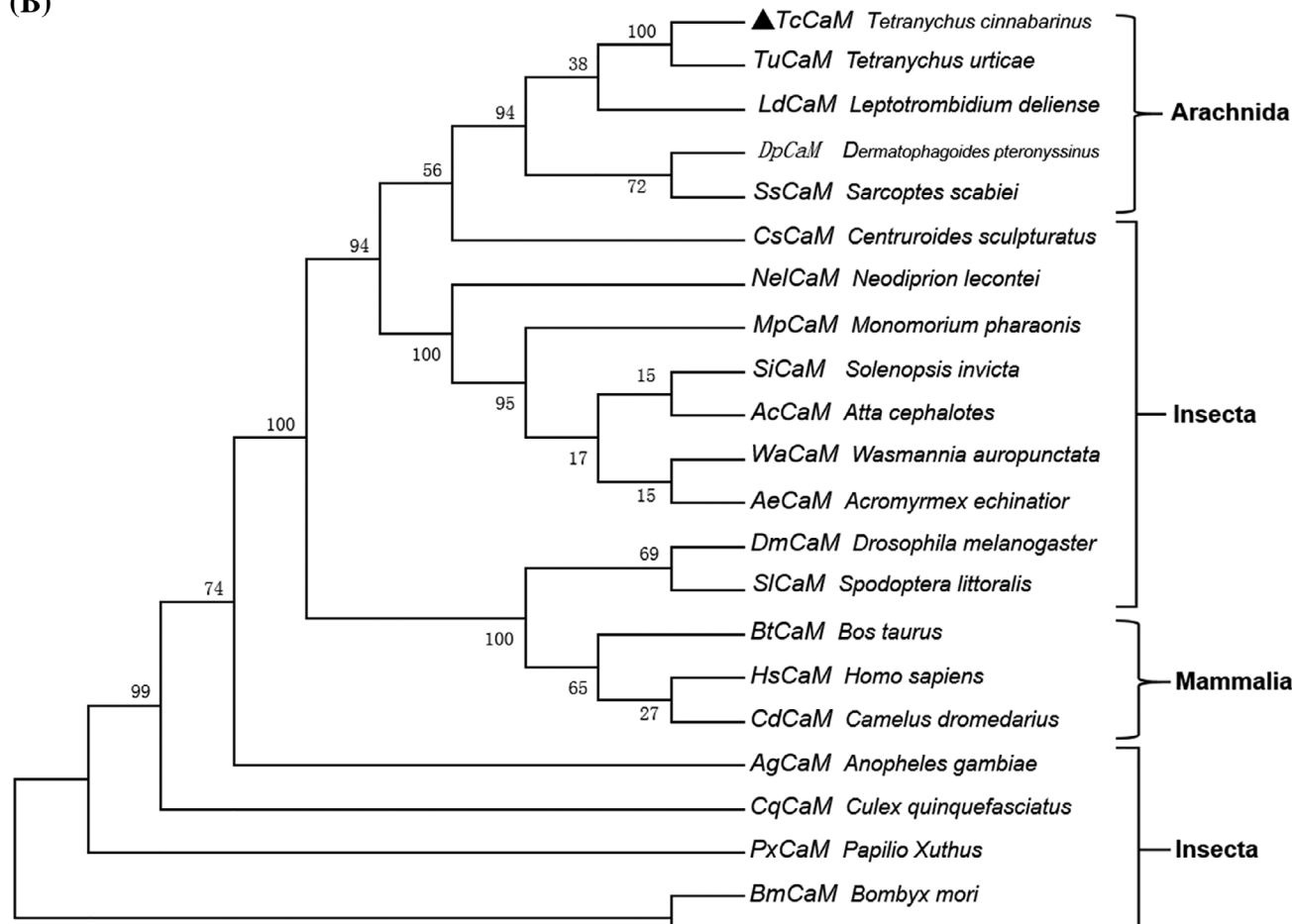
(B)

Figure 2. Nucleotide and deduced amino acid sequences of CaM gene (*TcCaM*) from the *Tetranychus cinnabarinus* (A); and phylogenic analysis of *TcCaMs* (B). (A) Nucleotide numbers are provided on the left. The four EF-hand domains are shaded. (B) Maximum likelihood tree constructed by MEGA 5.0. Phylogeny testing was conducted via the bootstrap method with 1000 replications. The sequences used for constructing the tree are listed in Supporting Information Table S2.

These results indicate that transcription of *TcCaM* in *T. cinnabarinus* was successfully silenced by RNAi in mites.

The PDE activation by CaM was determined in mites after 48 h of pretreatment with dsRNA. The results showed that the PDE activation by CaM was significantly decreased by 0.45-fold at 48 h post-treatment after *TcCaM* dsRNA feeding (109.41 nmol mg^{-1} min^{-1}) compared with feeding of DEPC–water or dsRNA–GFP (200.57 nmol mg^{-1} min^{-1} or 198.63 nmol mg^{-1} min^{-1}, respectively). However, no significant difference in activity was observed between the water and dsRNA–GFP controls (Fig. S4).

The susceptibilities to curcumin at 48 h after feeding *TcCaM* dsRNA were detected by slip-dip method. In LC$_{30}$ and LC$_{50}$ curcumin assays for 48 h, mortality was significantly decreased by 16% (from 30% to 14%) and 25% (from 55% to 30%), respectively, in mites fed *TcCaM* dsRNA compared with the control when *TcCaM* was knocked down by RNAi in mites (Fig. 3(C, D)). No significant
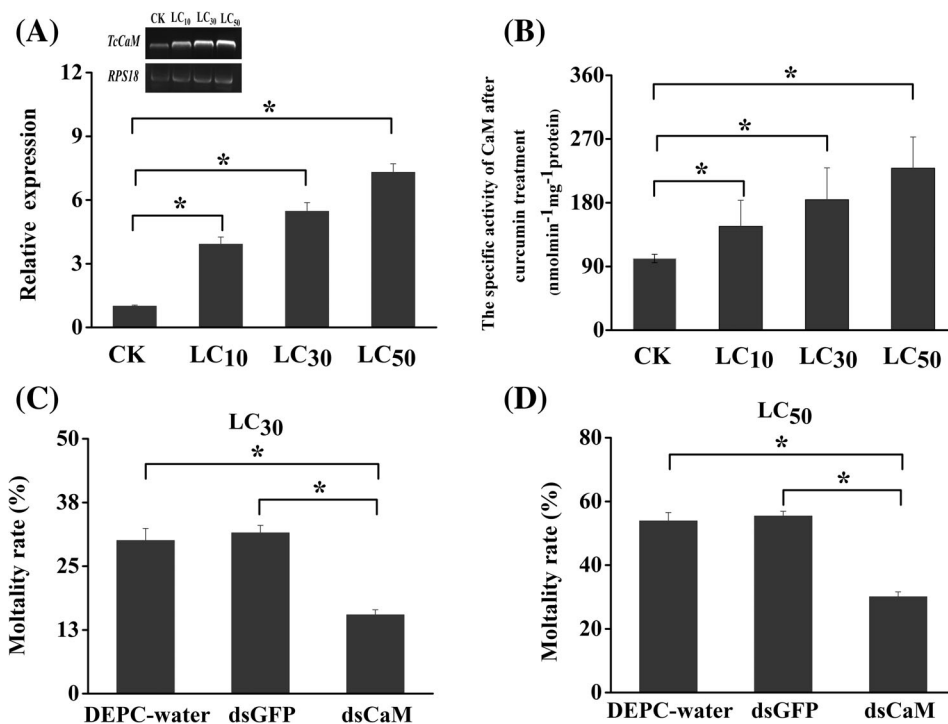
Figure 3. Expression profiles of *TcCaM* transcripts after curcumin treatment for 48 h at three different concentrations (A); the PDE activation by CaM was determined after curcumin treatment for 48 h (B); and knockdown of *TcCaM* expression reduced susceptibility to curcumin in mites (C, D). (A) Relative expression of the *TcCaM* of *Tetranychus cinnabarinus* exposed to 0.21, 1.23, and 2.64 mg L^{-1} curcumin (LC$_{10}$, LC$_{30}$ and LC$_{50}$) in 0.1% (*v/v*) Tween-80 and 3% (*v/v*) acetone at the adult stage for 48 h using a slip-dip bioassay were analyzed using RT-PCR and qPCR, respectively. (B) The PDE activation by CaM of *T. cinnabarinus* exposed to 0.21, 1.23, and 2.64 mg L^{-1} curcumin (LC$_{10}$, LC$_{30}$ and LC$_{50}$) in 0.1% (*v/v*) Tween-80 and 3% (*v/v*) acetone at the adult stage using a slip-dip bioassay was determined. (C) Mortality of *TcCaM*-silenced *T. cinnabarinus* to curcumin at LC$_{30}$. (D) Mortality of *TcCaM*-silenced *T. cinnabarinus* to curcumin at LC$_{50}$. Error bars represent the standard error of the calculated mean based on three biological replicates. Water containing 0.1% (*v/v*) Tween-80 and 3% (*v/v*) acetone was used as the control treatment (CK). An asterisk (*) on the error bar indicates a significant difference between the treatment and group CK according to *t*-tests, *P < 0.05. *RPS18* was used as the reference gene.

Table 1. Toxicity of curcumin against adult females of *Tetranychus cinnabarinus* after 48 h exposure time

Treatment	LC$_{50}$ (95% CI) mg L^{-1}	Slope ± standard error	χ^2 (df)	P	R
M	2.64 (1.68 ~ 6.08)	0.66 ± 0.12	0.87 (4)	0.51	—
M-T	9.61 (7.45 ~ 12.09)	2.02 ± 0.26	0.39 (3)	0.94	3.64

M, *T. cinnabarinus*; M-T, the mites pretreated with trifluoperazine (TFP) (58 µmol L^{-1}, IC$_{50}$ concentration of TFP); LC$_{50}$, median lethal concentration; 95% CI, 95% confidence interval; R, ratio = LC$_{50}$(M-T)/LC$_{50}$(M).

mortality difference existed between the water and dsRNA–*GFP* controls (Fig. 3(C, D)). These results indicate that *TcCaM* RNAi reduced the susceptibility of *T. cinnabarinus* to curcumin.

3.6 Bacterial expression and features of recombinant CaM

TcCaM was re-engineered for heterologous expression in *Escherichia coli*. In the whole-cell lysate, a novel specific band (about 19 kDa) was observed by SDS-PAGE analysis, and only one clear band was observed after purification (Fig. 4(A)). The specific activity of PDE activation by recombinant CaM was determined to be 263.4 nmol mg^{-1} min^{-1}, with a K_m value of 2.1 µmol L^{-1} (Table S3). The EC$_{50}$ value of curcumin-induced D-CaM fluorescence response, curcumin for PDE activation by D-CaM, curcumin for PDE and Ca^{2+}-Mg^{2+}-ATPase activation by CaM, and the IC$_{50}$ of TFP for PDE activation by CaM were determined. The results showed that the EC$_{50}$ value of curcumin-induced D-CaM

fluorescence response was 0.3 µmol L^{-1} (Fig. 4(B)); the EC$_{50}$ of curcumin for PDE activation by D-CaM was 224.8 µmol L^{-1} (Fig. 4(C)); the EC$_{50}$ of curcumin for PDE and Ca^{2+}-Mg^{2+}-ATPase activation by CaM were 234.2 µmol L^{-1} (Fig. 4(D)) and 136.1 µmol L^{-1} (Fig. 4(E)), respectively; the IC$_{50}$ of TFP for PDE activation by CaM was 58.7 µmol L^{-1} (Fig. 4(F)) (Table 2). Meanwhile, the EC$_{50}$ of curcumin for PDE activation by D-CaM was 224.8 µmol L^{-1}, which is similar to PDE-mediated curcumin's agonistic effect on CaM (234.2 µmol L^{-1}), indicating that dansyl chloride does not affect the activation of PDE by CaM.

3.7 Functional expression of *TcCaM* in Sf9 cells
A [Ca^{2+}]i assay in CaM- or GFP-expressing cells was performed *in vitro* to determine whether curcumin-induced calcium overload is mediated by CaM (Fig. 5(A, B)). The [Ca^{2+}]i level was detected by Fluo-4/AM fluorescence staining, and the Sf9 cells were incubated with curcumin at concentrations of 8.2 µmol L^{-1} (LC$_{50}$) for 48 h.
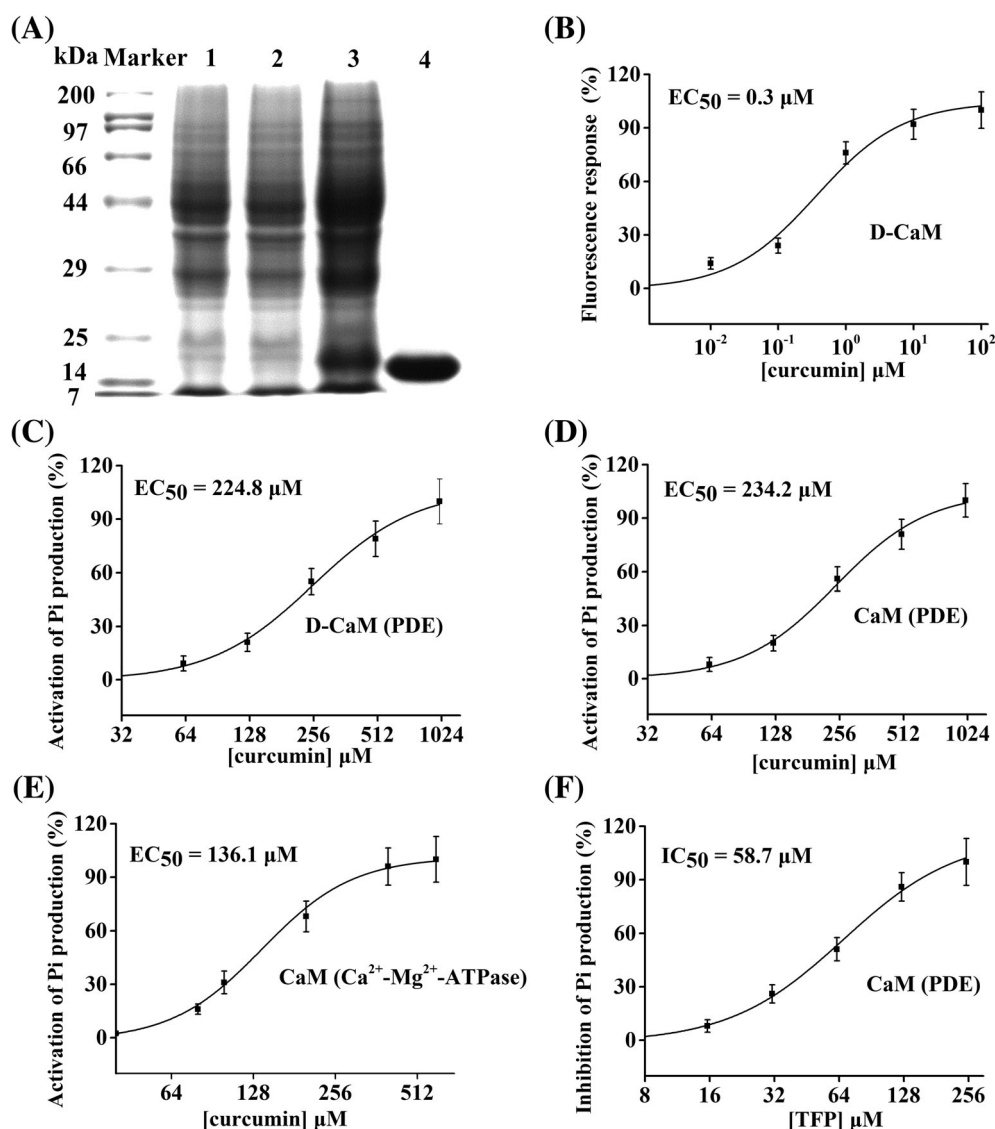
Figure 4. Effect of curcumin on recombinant CaM protein. (A) Expression of recombinant CaM protein by *Escherichia coli*. Lane 1: supernatant of pGEX-6p-1 (no insert). Lane 2: recombinant CaM without isopropyl β-D-1-thiogalactopyranoside (IPTG) induction. Lane 3: recombinant CaM with IPTG induction. Lane 4: purification of recombinant CaM. (B) The EC_{50} of curcumin-induced dansyl chloride-labeled CaM (D-CaM) fluorescence response. (C) The EC_{50} of curcumin for PDE activation by D-CaM. (D) The EC_{50} of curcumin for PDE activation by CaM. (E) The EC_{50} of curcumin for Ca^{2+}-Mg^{2+}-ATPase activation by CaM. (F) The IC_{50} of TFP for PDE activation by CaM. Error bars represent the standard error of the calculated mean based on three biological replicates. Data were fitted to theoretical curves using OriginPro 9.0 software with parameters shown in Table 2.

Table 2. A summary of half-maximal effective concentration (EC_{50}) and half-maximal inhibitory concentration (IC_{50}) on recombinant calmodulin (CaM)

Treatment	Method	EC_{50}/IC_{50} (95% CI) (μmol L^{-1})	Slope $\pm$ standard error	χ^2 (df)	P	R^2
Curcumin	D-CaM	0.3 (0.1 ~ 0.6)[a]	1.67 $\pm$ 0.13	2.1 (4)	0.41	0.95
Curcumin	D-CaM (PDE)	224.8 (178.1 ~ 285.4)[a]	4.74 $\pm$ 0.36	7.6 (4)	0.11	0.99
Curcumin	CaM (PDE)	234.2 (199.7 ~ 250.6)[a]	5.00 $\pm$ 0.38	6.4 (4)	0.17	0.99
Curcumin	CaM (Ca^{2+}-Mg^{2+}-ATPase)	136.1 (124.8 ~ 148.8)[a]	6.59 $\pm$ 0.51	2.5 (4)	0.65	0.99
TFP	CaM (PDE)	58.7 (53.5 ~ 60.0)[b]	4.99 $\pm$ 0.38	6.6 (4)	0.16	0.99

D-CaM, fluorescent labeling of CaM with dansyl chloride; D-CaM (PDE), phosphodiesterases (PDE) activation by dansyl chloride-labeled CaM; CaM (PDE), PDE activation by CaM; CaM (Ca^{2+}-Mg^{2+}-ATPase), Ca^{2+}-Mg^{2+}-ATPase activation by CaM; 95% CI, 95% confidence interval.
[a] EC_{50}.
[b] IC_{50}.

The results revealed [Ca^{2+}]i levels in CaM-expressing cells induced by curcumin were significantly higher (7.00-fold) than in GFP-expressing cells.

An assay of the recombinant CaM protein was then performed *in vitro* to examine the PDE activation by CaM (Fig. 5(C)). The results demonstrated that the PDE activation by CaM (379.26 nmol mg^{-1} min^{-1}) in the presence of cAMP was 14.36-fold higher compared with the effect of GFP (26.41 nmol mg^{-1} min^{-1}).

A cytotoxicity assay with MTT was also conducted to determine the toxicity of curcumin in CaM-expressing Sf9 cells (Fig. 5(D)), and the results revealed decreased cell viability due to the cytotoxic effects of curcumin in CaM-expressing cells compared with GFP-expressing cells. The LC$_{50}$ value of curcumin in GFP-expressing cells (8.21 μmol L^{-1}) was approximately 10.8-fold that in CaM-expressing cells (0.76 μmol L^{-1}) (Table S4).

3.8 Molecular docking

To examine the interaction between the curcumin ligand and *TcCaM* and evaluate the structure–activity relationship, molecular docking was conducted to assess the binding mode of curcumin within the binding pocket of *TcCaM*. The docking results of curcumin binding to *TcCaM* are shown in Table S5. The binding energy of curcumin was calculated to be 3.97 kcal mol^{-1}, which indicates that curcumin can be considered a specific ligand of *TcCaM*. Figure 6(E, F) shows the binding modes and orientations of curcumin with *TcCaM*, and two-dimensional interaction diagrams of curcumin with *TcCaM* are shown in Fig. 6(C). Five key amino acids (GLU131, MET141, ALA145, VAL161, and PHE109) interact with curcumin via hydrogen bonding and hydrophobic interactions

in the binding pocket of *TcCaM*. The hydrogen atoms of the hydroxyls at positions 1 and 7 of the benzene ring form a conventional hydrogen bond (–H…OC–, 1.81 Å and 1.75 Å) with GLU131 and MET141, respectively. In addition, the acidic residues LEU122, ASP140, ILE142, GLU144, LEU135, IEU129, PHE158, LEU162, and PRO165 interact with curcumin via Van der Waals interactions in the binding pocket of *TcCaM*. Curcumin also forms Pi–sulfur interactions with MET126.

4 DISCUSSION

To study the role of CaM in curcumin-mediated intracellular calcium overload, we used a specific inhibitor of CaM, TFP, to pre-treat cells.[25] Meanwhile, TFP also acts as a plasma membrane Ca^{2+}-ATPase (PMCA) blocker.[43, 44] The plasma membrane Ca^{2+}-ATPase (PMCA) pumps Ca^{2+} out of the cell to maintain cytosolic Ca^{2+} concentration at a level that is compatible with messenger function.[45] The concentration of nerve membrane Ca^{2+} is normally higher in the cytoplasm than that in the extracellular matrix; furthermore, Ca^{2+} is sequestered by Ca^{2+}-binding proteins (CaM), or by sarco/endoplasmic reticulum Ca^{2+} pumps (SERCA) or else extruded by Na^{+}/Ca^{2+} exchangers or PMCAs.[46] PMCAs exhibit cell-specific expression patterns and play an essential role in Ca^{2+} homeostasis in various cell types, including sensory neurons.[47–49] The inhibition of PMCAs in rat and fire salamander cilia by specific drugs, such as vanadate or carboxyeosin, suggests that PMCAs play a predominant role in Ca^{2+} clearance.[50] In this study, TFP inhibited the increase in [Ca^{2+}]i levels, and the TFP pre-treated Sf9 cells were resistant to curcumin-mediated increase in [Ca^{2+}]i levels, suggesting that curcumin-treated intracellular [Ca^{2+}]i overload may be mediated by CaM or PMCA.
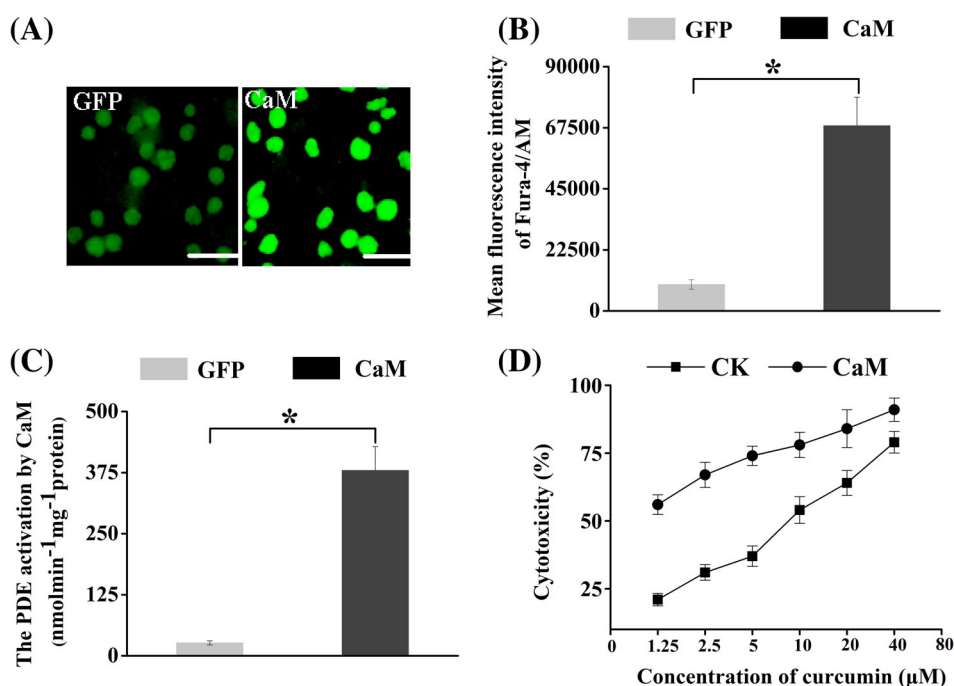

Figure 5. The intracellular [Ca^{2+}]i in GFP- and CaM-expressing cells exposed to curcumin (A, B); the PDE activation by CaM in recombinant enzymes expressing CaM toward the substrate of cAMP (C); and cytotoxicity of curcumin against CaM- and GFP-expressing cells (D). (A) The [Ca^{2+}]i level was detected by Fluo-4/AM fluorescence staining, and the Sf9 cells were incubated with curcumin at concentrations of 8.2 μmol L^{-1} (LC$_{50}$) for 48 h. (B) The bar chart indicates the mean fluorescence intensity of Fluo-4/AM in Sf9 cells. Positively stained calcium is shown as green zones in the captured images under a microscope. The percentage of viable cells was detected using MTT cytotoxicity assays. Error bars represent the standard error of the calculated mean based on three biological replicates. Asterisks (*) above the error bars indicate statistical differences determined by the independent samples *t*-test, *P < 0.01.
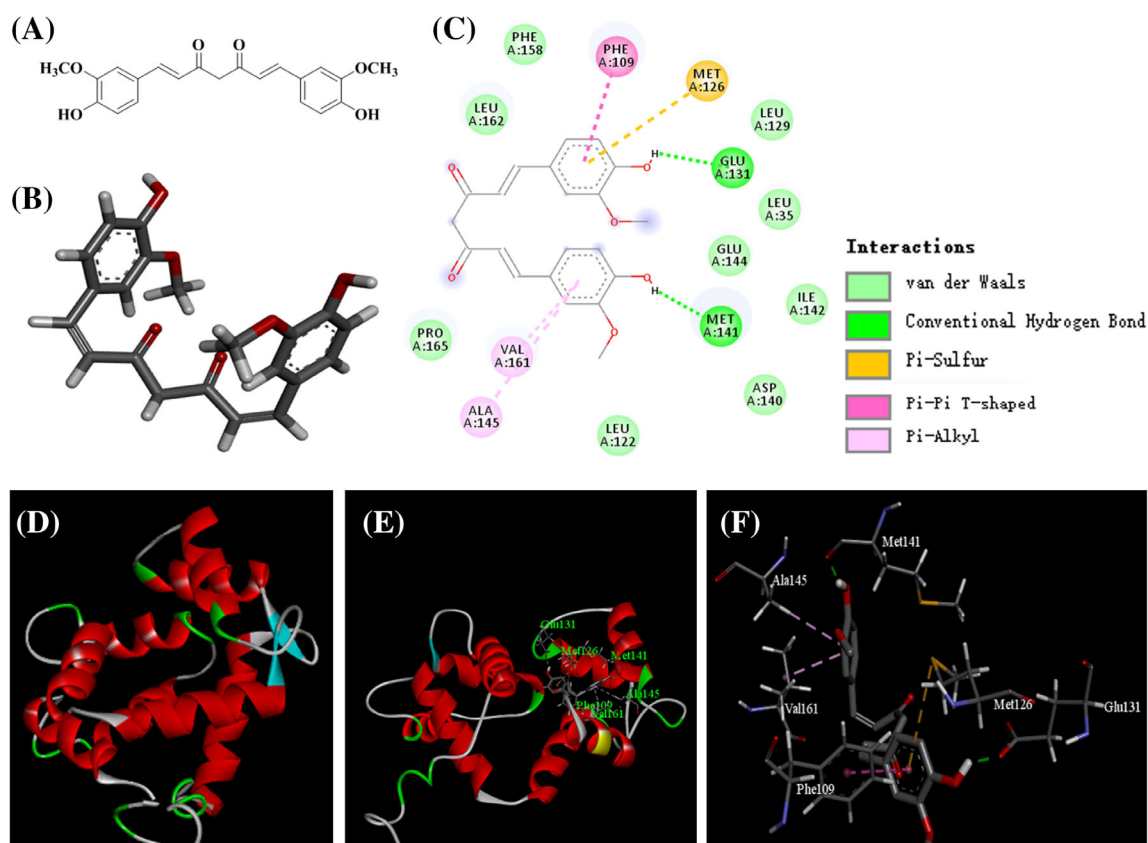
Figure 6. Molecular docking of CaM protein to curcumin. (A) Chemical structural formula of curcumin. (B) The cartoon representation of curcumin. Red regions represent oxygen atoms; gray regions represent carbon atoms. (C) The two-dimensional interactions scheme of curcumin to *TcCaM*. (D) Homology modeling 3D-structure of *TcCaM*. (E) Best conformation of curcumin docked to binding pocket of *TcCaM*. (F) The recognized binding modes and molecular interactions of the curcumin in the active site of *TcCaM*.

However, in our previous study, RNA-Seq analysis revealed that the LC_{50} dose of curcumin significantly increased expression of the CaM gene at 48 h (by 6.87-fold) compared with that of the control, indicating that CaM may play a key role in curcumin-induced intracellular $[Ca^{2+}]i$ overload.[16] It has been reported that elevation of $[Ca^{2+}]i$ induced by curcumin promotes apoptosis in tumor cells, including lung cancer cells,[51] hepatocellular carcinoma cells,[52] and mouse melanoma cells.[53] The continued increase in $[Ca^{2+}]i$ levels might mediate the activation of numerous Ca^{2+}-dependent events, and the CaM protein is a key calcium sensor that plays a vital role in the majority of calcium signaling.[54] Overall, these results show that activation of CaM expression has a key role in the mode of action of curcumin against *T. cinnabarinus*.

Here, a *CaM* gene from *T. cinnabarinus*, referred to as *TcCaM*, is characterized. The predicted amino acid sequence of the protein contains four EF-hand domains, embodying a 12-residue loop flanked by a 12-residue alpha-helical domain existing on both sides.[55] The six residues of the EF-hand motif at positions 1, 3, 5, 7, 9 and 12 are involved in Ca^{2+} binding, and position 12 offers two oxygen atoms for interaction between Ca^{2+} and glutamate or aspartate.[56] The conformational change of the EF-hand motif is induced by Ca^{2+} binding, which results in the activation or inactivation of target proteins.[55] In addition, transcript levels of *TcCaM* in *T. cinnabarinus* resemble those in *Echinococcus granulosus*,[57] being expressed in most developmental stages but rarely in the egg stage; this suggests that the *CaM* gene is critical for the development of mites.

In the present study, *TcCaM* gene transcript levels were significantly upregulated and the CaM protein was significantly activated in mites after curcumin exposure, indicating that the increase in activity of PDE activation by CaM protein in curcumin-exposed mites is possibly mediated by overexpression of the *CaM* gene. Therefore, to determine whether the increase in activity of PDE activation by CaM mediates the acaricidal mechanism of curcumin, TFP was applied to inhibit endogenous CaM function. Indeed, the results of toxicity assays indicated that the LC_{50} dose of curcumin against *T. cinnabarinus* increased 3.62-fold compared with that in the control, suggesting that inhibiting CaM function reduces the susceptibility of *T. cinnabarinus* to curcumin. Numerous studies have emphasized the significance of the widespread Ca^{2+}-binding protein CaM in the regulation of Ca^{2+} channels.[58] Dick *et al* reported that CaM senses the local Ca^{2+} signal via its N- and C-lobes and is attached to combining motifs in the C-lobe of the L-type Ca^{2+} channel α_1-subunit during Ca^{2+}-dependent facilitation (CDF) and Ca^{2+}-dependent inactivation (CDI) of channel activity.[59] Mutation of either of the Ca^{2+}-binding sites in CaM[60] or the CaM-binding motifs in the C-lobe of the L-type Ca^{2+} channel α_1-subunit[61] eliminates both CDF and CDI, indicating that CaM plays a key role in regulating Ca^{2+} channels under physiological conditions. In our study, $[Ca^{2+}]i$ levels in CaM-expressing cells induced by curcumin were higher than those in GFP-expressing cells (Fig. 5), suggesting that activation of CaM by curcumin is likely to induce intracellular calcium overload by promoting CDF or inhibition of CDI to cause excessive

activation of calcium signaling, thereby resulting in the death of mites. Nevertheless, the regulation of intracellular Ca^{2+} signaling is exceedingly complicated. Thus, the mechanism of Ca^{2+} overload that is mediated by overexpression of the *CaM* gene in curcumin-exposed mites needs further clarification.

Overexpression of the CaM gene highlights its importance in the mode of action of curcumin in mites.[16] Regardless, it remains unclear how overexpression of the *CaM* gene is connected with the acaricidal phenotype. To elucidate the acaricidal mechanisms of compounds, RNAi is considered to demonstrate the link between gene function and overexpression. Indeed, RNAi technology has been extensively used to identify or validate target genes of insecticides in insects and mites.[62,63] In this study, RNAi was conducted to decrease the transcript levels of the CaM gene such that changes in mortality after gene silencing could be detected. As latent targets for insecticides, alteration of in the expression levels of these genes has been shown to mediate insecticidal mechanisms in numerous pests.[64–66] A recent study reported that RNAi silencing of the glutamate receptor gene led to a reduction in the susceptibility of *Plutella xylostella* to abamectin.[64] Another study showed that RNAi-mediated overexpression of the G-protein-coupled neuropeptide receptor gene reduced the susceptibility of *T. cinnabarinus* to scopoletin.[26] These findings indicate that the transcript levels of target genes can be knocked down using RNAi and that the increase in transcript levels of target genes is a possible insecticidal mechanism. Similarly, our results from RNAi and toxicity tests indicated the involvement of CaM in the toxicity of curcumin towards *T. cinnabarinus*. In this study, the activity of PDE activation by CaM was significantly reduced and susceptibility to curcumin was decreased when *TcCaM* was downregulated via RNAi in LC_{50} and LC_{30} assays, indicating that RNAi-mediated overexpression of the *CaM* gene decreases the susceptibility of *T. cinnabarinus* to curcumin. Taken together, these results further suggest that the acaricidal activity of curcumin aganist *T. cinnabarinus* is mediated by overexpression of CaM.

In the current study, CaM was overexpressed in *Escherichia coli* and purified, and the properties of the recombinant CaM were characterized. The activity of PDE activation by recombinant CaM protein was approximately 2.6-fold greater than that of the crude extracts from mites (Table S3). In general, the enzymatic activities of recombinant proteins are higher compared with those of the natural crude enzyme isolated from organisms due to their higher purity and specificity. However, recombinant CaM did not possess significantly higher enzymatic activity than that of the natural protein from *T. cinnabarinus*, indicating a possible post-transcriptional modification lacking in the *Escherichia coli* system.[67] In contrast to the *Escherichia coli* system, the baculovirus expression system is appropriate in terms of post-transcriptional modification.[68] Thus, altering the expression system might be a good strategy to obtain recombinant CaM with increased activity, and a baculovirus expression system was used for the CaM gene expression in this study. Indeed, the activity of PDE activation by CaM protein obtained from the baculovirus expression system was increased by more than 3.7-fold compared to that of the crude extract from *T. cinnabarinus* (Fig. 5).

CaM itself does not display any catalytic activity.[69] However, the activation of many target enzymes, including PDE, Ca^{2+}-Mg^{2+}-ATPase, myosin kinase, phosphatase, phospholipase A_2, NAD kinase, NAD oxidoreductase, was mediated by CaM *in vivo*.[20] Thus, we used PDE and Ca^{2+}-Mg^{2+}-ATPase to evaluate the curcumin-mediated CaM protein activity, respectively. In this study, the

EC_{50} of curcumin for PDE and Ca^{2+}-Mg^{2+}-ATPase activation by CaM were 234.2 μmol L^{-1} and 136.1 μmol L^{-1}, respectively, indicating the mechanism by which CaM activates its target protein may be different. However, the LC_{50} value of curcumin against mites and CaM-expressing Sf9 cells were 8.2 μmol L^{-1} and 0.76 μmol L^{-1}, respectively, which were markedly lower than that of PDE (28.6- and 308.2-fold, respectively) and Ca^{2+}-Mg^{2+}-ATPase (16.6- and 8.1-fold, respectively)-mediated curcumin agonistic effect on recombinant CaM (234.2 μmol L^{-1} and 179.1 μmol L^{-1}, respectively), respectively, suggesting that the indirect agonistic effect of curcumin on CaM mediated by the target enzyme may not represent the actual activation of curcumin on CaM, which may lead to differences in the agonistic effect of curcumin on CaM *in vivo* and *in vitro*. In short, the CaM activation by target enzyme mediated curcumin may not explain the toxic effect of curcumin on Sf9 cells/mites.

CaM regulates the activity of its target enzymes through the change of its conformation.[70] It was reported that the inactivation of CaM by TFP may be due to the change of the tertiary structure of CaM from an elongated dumb-bell, with exposed hydrophobic surfaces, to a compact globular form which can no longer interact with its target enzymes.[71] Thus, the direct interaction between curcumin and CaM was evaluated by studying the change in the fluorescence intensity of D-CaM caused by curcumin. In this study, the EC_{50} value of curcumin-induced D-CaM fluorescence response *in vitro* is about 0.3 μmol L^{-1}, which is similar to curcumin against CaM-expressing Sf9 cells (0.76 μmol L^{-1}) *in vivo*, indicating that the conformational change of CaM induced by curcumin may represent the agonistic effect of curcumin on CaM *in vivo* and *in vitro*. Does a single polypeptide sequence encode a single protein conformation? The case of CaM, a central coordinator for many proteins that are influenced by calcium dynamics, clearly indicates that the conformation of a protein changes depending on its environment. Various CaM binding partners dictate the 3D structure of CaM mainly by changing the orientation of the two CaM globular lobes.[70] Furthermore, high-resolution crystallographic studies revealed significant rearrangement of EF-hand helices within each CaM lobe to adjust its conformation for optimal binding with a target.[72] Meanwhile, curcumin induced intracellular $[Ca^{2+}]i$ overload of Sf9 cells was confirmed in our study. Hence, the conformational change of CaM induced by curcumin may induce interactions between sites on the target proteins and sites on CaM that change conformation in response to calcium signaling. In summary, the acaricidal activity of curcumin may be due to the disruption of intracellular Ca^{2+} homeostasis mediated by curcumin-induced CaM conformation changes.

Molecular docking and homology modeling of target proteins are novel and effective approaches to characterize conformational protein–ligand interaction patterns.[4, 41] On the basis of its identity with the main sequence of the target protein *TcCaM*, the crystal structure of the bovine brain Ca^{2+}/calmodulin complex (PDB ID code: 1PRW) was retrieved from Protein Data Bank (PDB, available online: https://www.rcsb.org/structure/1PRW) and used as the template for homology modeling. The complex is a slender dumbbell-shaped molecule with two structurally analogous globular domains, termed EF-hands, and two flexible hydrophobic binding pockets typical of the CaM protein,[73] confirming that the CaM protein indeed has the structural capacity to interact with and bind curcumin. Binding and activation of the recombinant CaM protein by curcumin were also confirmed by our experiments. In our docking results, the critical residues of the C-lobe globular domain in the binding pocket of the CaM protein, such

as GLU131, MET141, ALA145, VAL161, and PHE109, interact with curcumin via hydrogen bonding and hydrophobic interactions, showing that the C-lobe globular domain of the active site is favorable for interactions with curcumin. Similar results were obtained from the crystal structure data of CaM–drug complexes, revealing that the C-lobe globular domain is a unique site for binding of the anti-CaM drug TFP.[74] However, melittin, a 26-residue peptide antagonist of CaM, has been reported to interact with both the C- and N-lobe domains.[75] These results demonstrate that the C- and N-lobe globular domains of the CaM binding sites are responsible for the functions of different drugs; activation of the recombinant CaM protein by curcumin may have occurred through the C-lobe globular domain in the CaM active site.

5 CONCLUSION

In summary, this study offers basic information on the sequence, phylogeny, and expression pattern of the CaM gene in *T. cinnabarinus*. The detection of specific expression patterns demonstrated that curcumin exposure significantly upregulated *TcCaM* expression. The inhibition of CaM function by the anti-CaM drug TFP and RNAi against the CaM gene decreased the sensitivity of *T. cinnabarinus* to curcumin. Moreover, the TFP pre-treated Sf9 cells were resistant to curcumin-mediated increase in $[Ca^{2+}]i$ levels, and the $[Ca^{2+}]i$ levels in CaM-expressing Sf9 cells induced by curcumin were higher than those in GFP-expressing cells. More importantly, our results showed that the recombinant CaM protein can be directly activated by curcumin via inducing its conformational changes. These results demonstrate that the mode of action of curcumin against mites may be via activating CaM function, and thereby disrupting intracellular Ca^{2+} homeostasis in *T. cinnabarinus*. This study promotes our understanding of the molecular mechanism of curcumin against mites and clarifies strategies that might be used to control pest mites.

ACKNOWLEDGEMENTS

SUPPORTING INFORMATION

Supporting information may be found in the online version of this article.

REFERENCES

1 Zhang Y, Zhang Z, Yutaka S, Liu Q and Ji J, On the causes of mite pest outbreaks in mono- and poly-cultured moso bamboo forests. *Chin J Appl Ecol* **15**:1161–1165 (2004).
2 Çakmak I, Başpinar H and Madanlar N, Control of the carmine spider mite *Tetranychus cinnabarinus* boisduval by the predatory mite *Phytoseiulus persimilis* (Athias-Henriot) in protected strawberries in Aydin, Tukey. *Turk J Agric For* **29**:259–265 (2005).
3 Sarwar M, Management of spider mite *Tetranychus cinnabarinus* (Boisduval) (Tetranychidae) infestation in cotton by releasing the predatory mite *Neoseiulus pseudolongispinosus* (Xin, Liang and Ke) (Phytoseiidae). *Biol Control* **65**:37–42 (2013).
4 Hou QL, Luo JX, Zhang BC, Jiang GF, Ding W and Zhang YQ, 3D-QSAR and molecular docking studies on the TcPMCA1-mediated detoxification of scopoletin and coumarin derivatives. *Int J Mol Sci* **18**:1380 (2017).
5 Hidaka H, Ishiko T, Furuhashi T, Kamohara H, Suzuki S, Miyazaki M et al., Curcumin inhibits interleukin 8 production and enhances interleukin 8 receptor expression on the cell surface: impact on human pancreatic carcinoma cell growth by autocrine regulation. *Cancer* **95**:1206–1214 (2010).
6 Li N, Chen X, Liao J, Yang G, Wang S, Josephson Y et al., Inhibition of 7,12-dimethylbenz[a]anthracene (DMBA)-induced oral carcinogenesis in hamsters by tea and curcumin. *Carcinogenesis* **23**:1307–1313 (2002).
7 Zhang YQ, Wei D and Zhao ZM, Biological activities of curcuminoids against *Tetranychus cinnabarinus* Boisduval (Acari:Tetranychidae). *Acta Ent Sin* **50**:1304–1308 (2007).
8 Tripathi AK, Prajapati V, Verma N, Bahl JR, Bansal RP, Khanuja SPS et al., Bioactivities of the leaf essential oil of *Curcuma longa* on three species of stored-product beetles (Coleoptera). *J Econ Entomol* **95**:183–189 (2002).
9 Martins CVB, Silva DLD, Neres ATM, Magalhães TFF, Watanabe GA, Modolo LV et al., Curcumin as a promising antifungal of clinical interest. *J Antimicrob Chemother* **63**:337 (2009).
10 Brouet I and Ohshima H, Curcumin, an anti-tumour promoter and anti-inflammatory agent, inhibits induction of nitric oxide synthase in activated macrophages. *Biochem Biophys Res Commun* **206**:533–540 (1995).
11 Sharma OP, Antioxidant activity of curcumin and related compounds. *Biochem Pharmacol* **25**:1811–1812 (1976).
12 Swatson WS, Katohkurasawa M, Shaulsky G and Alexander S, Curcumin affects gene expression and reactive oxygen species via a PKA dependent mechanism in *Dictyostelium discoideum*. *PLos One* **12**:e0187562 (2017).
13 Mukhopadhyay A, Bueso-Ramos C, Chatterjee D, Pantazis P and Aggarwal BB, Curcumin downregulates cell survival mechanisms in human prostate cancer cell lines. *Oncogene* **20**:7597–7609 (2001).
14 Zhang YQ, Ding W, Zhao ZM, Wu J and Fan YH, Acaricidal bioactivity of different growth period *Artemisia annua* extracts against *Tetranychus cinnabarinus*. *Chin J Ecol* **26**:1969–1973 (2007).
15 Luo JX, Ding W, Zhang YQ, Yang ZG, Yang LI and Ding LJ, Acaricidal activity of bisdemethoxycurcumin and N-methylpyrazolebisdemethoxycurcumin against *Tetranychus cinnabarinus* (Boisduval) and their effects on enzymes activity in the mite. *Sci Agric Sin* **46**:2833–2844 (2013).
16 Liu X, Wu D, Zhang Y, Hong Z, Lai T and Wei D, RNA-seq analysis reveals candidate targets for curcumin against *Tetranychus cinnabarinus*. *Biomed Res Int* **2016**:1–10 (2016).
17 Berridge MJ, Bootman MD and Roderick HL, Calcium signalling: dynamics, homeostasis and remodelling. *Nat Rev Mol Cell Biol* **4**:517–529 (2003).
18 Pang ZP, Cao P, Xu W and Südhof TC, Calmodulin controls synaptic strength via presynaptic activation of calmodulin kinase II. *J Neurosci* **30**:4132–4142 (2010).
19 Shirasaki Y, Kanazawa Y, Morishima Y and Makino M, Involvement of calmodulin in neuronal cell death. *Brain Res* **1083**:189–195 (2006).
20 Shim JS, Lee J, Park HJ, Park SJ and Kwon HJ, A new curcumin derivative, HBC, interferes with the cell cycle progression of colon cancer cells via antagonization of the Ca/calmodulin function. *Chem Biol* **11**:1455–1463 (2004).
21 Babu YS, Sack JS, Greenhough TJ, Bugg CE, Means AR and Cook WJ, Three-dimensional structure of calmodulin. *Nature* **315**:37–40 (1985).
22 Copley RR, Schultz J, Ponting CP and Bork P, Protein families in multicellular organisms. *Curr Opin Struct Biol* **9**:408–415 (1999).
23 Dolmetsch RE, Pajvani U, Fife K, Spotts JM and Greenberg ME, Signaling to the nucleus by an L-type calcium channel–calmodulin complex through the MAP kinase pathway. *Science* **294**:333–339 (2001).
24 Duan JY, Li-Ming DU, Hao WU, Yuan LH and Gang G, Preliminary study of action mechanism of tomatine toxicity to *Helicoverpa armigera*. *Acta Bot Boreali-Occidentalia Sin* **26**:117–120 (2006).
25 Iwanaga M, Dohmae N, Fonagy A, Takio K, Kawasaki H, Maeda S et al., Isolation and characterization of calmodulin in the pheromone gland of the silkworm, *Bombyx mori*. *Comp Biochem Phys B* **120**:761–767 (1998).
26 Zhou H, Zhang YQ, Lai T, Liu XJ, Guo FY, Guo T et al., Acaricidal mechanism of scopoletin against *Tetranychus cinnabarinus*. *Front Physiol* **10**:1–17 (2019).
27 Busvine JR, *Recommended methods for measurement of pest resistance to pesticides*. Food and Agricultural Organization of the United Nations, Rome (1980).

28 Zhou H, Zhang YQ, Lai T, Wang D, Liu JL, Guo FY *et al.*, Silencing Chitinase genes increases susceptibility of *Tetranychus cinnabarinus* (Boisduval) to scopoletin. *Biomed Res Int* **7**:1–13 (2017).

29 Michel AP, Mian MA, Davila-Olivas NH and Cañas LA, Detached leaf and whole plant assays for soybean aphid resistance: differential responses among resistance sources and biotypes. *J Econ Entomol* **103**:949–957 (2010).

30 Hill CB, Li Y and Hartman GL, Resistance to the soybean aphid in soybean germplasm. *Crop Sci* **44**:98–106 (2004).

31 Bansal R, Hulbert S, Schemerhorn B, Reese JC, Whitworth RJ, Stuart JJ *et al.*, Hessian fly-associated bacteria: transmission, essentiality, and composition. *PLoS One* **6**:e23170 (2011).

32 Tamura K, Peterson D, Peterson N, Stecher G, Nei M and Kumar S, MEGA5: molecular evolutionary genetics analysis using maximum likelihood, evolutionary distance, and maximum parsimony methods. *Mol Biol Evol* **28**:2731–2739 (2011).

33 Misener S and Krawetz SA, *Bioinformatics Methods and Protocols*. Humana Press, Totowa, NJ (2000).

34 Sun W, Jin Y, He L, Lu WC and Li M, Suitable reference gene selection for different strains and developmental stages of the carmine spider mite, *Tetranychus cinnabarinus*, using quantitative real-time PCR. *J Insect Sci* **10**:208–208 (2010).

35 Livak KJ and Schmittgen TD, Analysis of relative gene expression data using real-time quantitative PCR and the 2(−delta delta C(T)) method. *Methods* **25**:402–408 (2001).

36 He G, Guo F, Zhu T, Shao D, Feng R, Yin D *et al.*, Lobe-related concentration- and Ca²⁺-dependent interactions of calmodulin with C- and N-terminal tails of the Ca$_V$1.2 channel. *J Physiol Sci* **63**:345–353 (2013).

37 Dedman JR and Kaetzel MA, Calmodulin purification and fluorescent labeling. *Method Enzymol* **102**:1–8 (1983).

38 Garg UC, Rai N, Singh Y, Dhaunsi GS, Sidhu GS, Ganguly NK *et al.*, A spectrophotometric method for calmodulin assay. *Biotechniques* **6**:294–296 (1988).

39 Lanzetta PA, Alvarez LJ, Reinach PS and Candia OA, An improved assay for nanomole amounts of inorganic phosphate. *Anal Biochem* **100**:95–97 (1979).

40 Benaim G, Zurini M and Carafoli E, Different conformational states of the purified Ca²⁺-ATPase of the erythrocyte plasma membrane revealed by controlled trypsin proteolysis. *J Biol Chem* **259**:8471–8477 (1984).

41 Luo JX, Lai T, Guo T, Chen F, Zhang L, Ding W *et al.*, Synthesis and acaricidal activities of scopoletin phenolic ether derivatives: QSAR, molecular docking study and in silico ADME predictions. *Molecules* **23**:995 (2018).

42 Ao J, Gao L, Yuan T and Jiang G, Interaction mechanisms between organic UV filters and bovine serum albumin as determined by comprehensive spectroscopy exploration and molecular docking. *Chemosphere* **119**:590–600 (2015).

43 Bhatnagar K and Singh VP, Ca²⁺ dependence and inhibitory effects of trifluoperazine on plasma membrane ATPase of thermoactinomyces vulgaris. *Curr Microbiol* **49**:28–31 (2004).

44 Scharff O and Foder B, Effect of trifluoperazine, compound 48/80, TMB-8 and verapamil on the rate of calmodulin binding to erythrocyte Ca²⁺-ATPase. *Biochim Biophys Acta* **772**:29–36 (1984).

45 Penniston JT and Enyedi A, Modulation of the plasma membrane Ca²⁺ pump. *J Membr Biol* **165**:101–109 (1998).

46 Carafoli E, The calcium pumping ATPase of the plasma membrane. *Annu Rev Physiol* **53**:531–547 (1991).

47 Krizaj D, Steven JD, Johnson J, Strehler EE and Copenhagen DR, Cell-specific expression of plasma membrane calcium ATPase isoforms in retinal neurons. *J Comput Neurol* **451**:1–21 (2002).

48 Pottorf WJ and Thayer SA, Transient rise in intracellular calcium produces a long-lasting increase in plasma membrane calcium pump activity in rat sensory neurons. *J Neurochem* **83**:1002–1008 (2002).

49 Zenisek D and Matthews G, The role of mitochondria in presynaptic calcium handling at a ribbon synapse. *Neuron* **25**:229–237 (2000).

50 Castillo K, Delgado R and Bacigalupo J, Plasma membrane Ca²⁺-ATPase in the cilia of olfactory receptor neurons: possible role in Ca²⁺ clearance. *Eur J Neurosci* **26**:2524–2531 (2007).

51 Xu X, Chen D, Ye B, Zhong F and Chen G, Curcumin induces the apoptosis of non-small cell lung cancer cells through a calcium signaling pathway. *Int J Mol Med* **35**:1610–1616 (2015).

52 Wang WH, Chiang IT, Ding K, Chung JG and Hwang JJ, Curcumin-induced apoptosis in human hepatocellular carcinoma J5 cells:

critical role of Ca²⁺-dependent pathway. *Evidence-Based Complementary Altern Med* **12**:512907 (2012).

53 Bakhshi J, Weinstein L, Poksay KS, Nishinaga B, Bredesen DE and Rao RV, Coupling endoplasmic reticulum stress to the cell death program in mouse melanoma cells: effect of curcumin. *Apoptosis* **13**:904–914 (2008).

54 Chin D and Means AR, Calmodulin: a prototypical calcium sensor. *Trends Cell Biol* **10**:322–328 (2000).

55 Yap K, Ames JB, Swindells MB and Ikura M, Diversity of conformational states and changes within the EF-hand protein superfamily. *Proteins* **37**:499–507 (2015).

56 Kawasaki H and Kretsinger RH, Structural and functional diversity of EF-hand proteins: evolutionary perspectives. *Protein Sci* **26**:1898–1920 (2017).

57 Ning W, Zhong X, Song X, Gu X, Lai W, Yue X *et al.*, Molecular and biochemical characterization of calmodulin from *Echinococcus granulosus*. *Parasite Vector* **10**:597 (2017).

58 Gulati P, Gaspers LD, Dann SG, Joaquin M, Nobukuni T, Natt F *et al.*, Amino acids activate mTOR Complex1 via Ca²⁺/CaM signaling to hVps34. *Cell Metab* **7**:456–465 (2008).

59 Dick IE, Tadross MR, Haoya L, Hock TL, Wanjun Y and Yue DT, A modular switch for spatial Ca²⁺ selectivity in the calmodulin regulation of Ca$_V$ channels. *Nature* **451**:830–834 (2008).

60 Demaria CD, Soong TW, Alseikhan BA, Alvania RS and Yue DT, Calmodulin bifurcates the local Ca²⁺ signal that modulates P/Q-type Ca²⁺ channels. *Nature* **411**:484–489 (2001).

61 Zühlke RD, Pitt GS, Tsien RW and Reuter H, Ca²⁺-sensitive inactivation and facilitation of L-type Ca²⁺ channels both depend on specific amino acid residues in a consensus calmodulin-binding motif in the α1C subunit. *J Biol Chem* **275**:21121–21129 (2000).

62 Xu ZF, Wu Q, Xu Q and He L, Functional analysis reveals glutamate-gated chloride and γ-amino butyric acid channels as targets of avermectins in the carmine spider mite. *Toxicol Sci* **155**:258–269 (2016).

63 Wei P, Li J, Liu X, Nan C, Shi L, Zhang Y *et al.*, Functional analysis of four up-regulated carboxylesterase genes associated with fenpropathrin resistance in *Tetranychus cinnabarinus* (Boisduval). *Pest Manag Sci* **75**:252–261 (2018).

64 Shi XZ, Guo ZJ, Zhu X, Wang SL, Xu BY, Xie W *et al.*, RNA interference of the inhibitory glutamate receptor in *Plutella xylostella* (Lepidoptera: Plutellidae). *Acta Ent Sin* **55**:1331–1336 (2012).

65 Rinkevich FD and Scott JG, Limitations of RNAi of α6 nicotinic acetylcholine receptor subunits for assessing the in vivo sensitivity to spinosad. *Insect Sci* **20**:101–108 (2013).

66 Wan PJ, Guo WY, Yang Y, Lü FG, Lu WP and Li GQ, RNAi suppression of the ryanodine receptor gene results in decreased susceptibility to chlorantraniliprole in Colorado potato beetle *Leptinotarsa decemlineata*. *J Insect Physiol* **63**:48–55 (2014).

67 Gary W and Roy J, Post-translational modifications in the context of therapeutic proteins. *Nat Biotechnol* **24**:1241–1252 (2006).

68 Shen XM, Liao CY, Lu XP, Zhe W, Wang JJ and Wei D, Involvement of three esterase genes from *Panonychus citri* (McGregor) in fenpropathrin resistance. *Int J Mol Sci* **17**:1–15 (2016).

69 Gong D, Chi X, Wei J, Zhou G, Huang G, Zhang L *et al.*, Modulation of cardiac ryanodine receptor 2 by calmodulin. *Nature* **361**:1112–1115 (2019).

70 Hoeflich KP and Ikura M, Calmodulin in action: diversity in target recognition and activation mechanisms. *Cell* **108**:739–742 (2002).

71 Vandonselaar M, Hickie RA, Quail W and Delbaere LTJ, Trifluoperazine-induced conformational change in Ca²⁺-calmodulin. *Nat Struct Biol* **1**:795–801 (1994).

72 Kurokawa H, Osawa M, Kurihara H, Katayama N, Tokumitsu H, Swindells MB *et al.*, Target-induced conformational adaptation of calmodulin revealed by the crystal structure of a complex with nematode Ca²⁺/calmodulin-dependent kinase kinase peptide. *J Mol Biol* **312**:59–68 (2001).

73 Fallon JL and Quiocho FA, A closed compact structure of native Ca²⁺-calmodulin. *Structure* **11**:1303–1307 (2003).

74 Vertessy BG, Harmat V, Cskei Z, Náray-Szabó G, Orosz F and Ovádi J, Simultaneous binding of drugs with different chemical structures to Ca²⁺-calmodulin: crystallographic and spectroscopic studies. *Biochemistry* **37**:15300–15310 (1998).

75 Steiner RF, Albaugh S, Fenselau C, Murphy C and Vestling M, A mass spectrometry method for mapping the interface topography of interacting proteins, illustrated by the melittin-calmodulin system. *Anal Biochem* **196**:120–125 (1991).